Irradiation-induced hardening of Zircaloy-2 at room temperature under external stress conditions

XUE, Luwei
Interdisciplinary Graduate School of Engineering Sciences, Kyushu University

WATANABE, Hideo
Research Institute for Applied Mechanics, Kyushu University

https://doi.org/10.5109/7157991

出版情報：Proceedings of International Exchange and Innovation Conference on Engineering & Sciences (IEICES). 9, pp.287-292, 2023-10-19. 九州大学大学院総合理工学府
バージョン：

Irradiation-induced hardening of Zircaloy-2 at room temperature under external stress conditions

Luwei XUE[1, *], Hideo WATANABE[2]
[1] Interdisciplinary Graduate School of Engineering Sciences, Kyushu University
[2] Research Institute for Applied Mechanics, Kyushu University
*Corresponding author email: xue.luwei.202@s.kyushu-u.ac.jp

Abstract: *The irradiation-induced hardening behavior of Zircaloy-2 under irradiation with 3.2 MeV Ni^{3+} ions at room temperature (RT) with stress conditions was investigated using transmission electron microscope (TEM) examination and nanoindentation measurements. The results indicated that the impact of external tensile stress on the hardening of unirradiated samples was not significant. Although stress-induced dislocation lines were observed in samples stressed above 450 MPa, they were unevenly distributed and not dense enough to cause significant changes in hardness.*
Samples subjected to 1 dpa irradiation under stress exhibited a noticeable increase in hardness, but the extent of hardening remained nearly unchanged across different stress levels, suggesting a minor influence of external tensile stress. This study offers insights into the irradiation-induced hardening behavior of Zircaloy-2 subjected to a 1 dpa irradiation under the influence of external stress conditions at room temperature.

Keywords: Zirconium alloys; Irradiation-induced hardening; External tensile stress; Dislocations

1. INTRODUCTION

Zirconium alloys are critical materials within boiling water reactors (BWRs) owing to their exceptional nuclear properties, which include excellent corrosion resistance, high strength, toughness, and low neutron absorption. These properties make them the ideal choice for fuel cladding tubes that encase nuclear fuel [1-3]. However, during prolonged reactor operation, these cladding materials are exposed to harsh conditions, which include continuous interaction with cooling water, as well as be subjected to mechanical stresses brought on by component deformation and tensile strains brought on by the thermal expansion of the UO_2 fuel pellets. [4-5]. In such a service environment, cladding must withstand simultaneous exposure to neutron irradiation, mechanical stress, and corrosion due to water or steam.
Significant phenomena are caused by changes in the microstructure of materials induced by irradiation, including the creation of point defects, nucleation of dislocation loops, precipitate dissolution, and the redistribution of alloying elements [6-7]. These include modifications to the material's dimensions, a rise in hardness, and irradiation embrittlement, all of which pose a threat to the safety and lifetime of nuclear plants [3, 8-9].
Understanding the irradiation hardening behavior is crucial for ensuring the secure and enduring operation of nuclear reactors. Previous studies have primarily focused on the early stages of irradiation hardening, where significant changes in hardness were observed [10-13]. However, due to practical limitations in reproducing in-reactor conditions in experimental setups, a comprehensive examination of the combined impact of external stress and irradiation on the hardening behavior is lacking.
To address these challenges and gain a deeper understanding of the irradiation hardening mechanism, this study explores the impact of external tensile stress on the irradiation-induced hardening of Zircaloy-2 under 3.2 MeV Ni^{3+} ion irradiation. Given the advantages of economic efficiency and safety, numerous studies have employed ion irradiation as a means of simulating the neutron irradiation process, thereby facilitating the observation of comparable radiation phenomena. [14-15]. The experimental approach involves conducting transmission electron microscope (TEM) examinations and nanoindentation measurements to characterize the microstructural evolution and hardness changes.
This study investigates the impact of stress on the hardness of unirradiated samples through Vickers hardness tests and microstructural observations using TEM. Subsequently, ion irradiation is conducted at room temperature with varying levels of applied stress. Nanoindentation measurements are performed before and after irradiation to quantify the hardness changes in response to both stress and radiation. The aim of this research is to acquire a deeper understanding of how stress conditions impact the irradiation hardening behavior of Zircaloy-2 at room temperature.

2. EXPERIMENTAL METHOD

2.1 Sample preparation

This study utilized Zircaloy-2, characterized by an alloy composition of Zr-1.38Sn-0.15-Fe-0.09Cr-0.05Ni (wt.%).
Cold rolling was initially used to create thin sheets with an initial thickness of about 0.13 mm, which were then punched to create tensile samples. Fig. 1(a) and (b) depict the tensile sample's size, which include a nominal length of 4.9mm.
To attain an ultimate thickness of 0.1 mm, the tensile samples underwent mechanical grinding using abrasive papers ranging from #800 to #2000 grit, and diamond sandpaper with #8000 grit. Subsequently, a 0.3 μm Al_2O_3 suspension was used to achieve a fine mirror surface. Fig. 1(c) displays the surface appearance after polishing.
After the mechanical thinning process, the prepared samples underwent meticulous cleaning. They were immersed in acetone initially to remove any impurities,

followed by a final cleaning with ethanol in an ultrasonic bath.

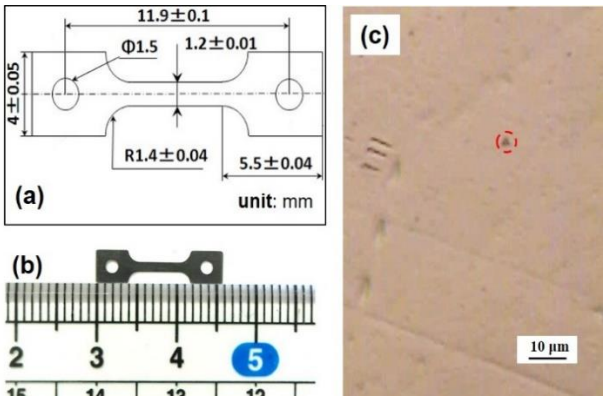

Fig. 1 Schematic illustrations of (a) the tensile sample, (b) the sample photograph, and (c) the surface of the sample after polishing

To mitigate residual stresses introduced during processing and enhance material homogeneity, the samples underwent annealing at 630 °C for a duration of 2 hours, followed by air-cooling to room temperature.

2.2 Ni^{3+} ion irradiation

Utilizing the tandem accelerator at Kyushu University [16], irradiation involving Ni^{3+} ions took place under room temperature conditions. The estimation of damage was derived from the calculation utilizing the stopping and range of ions in matter (SRIM) methodology [17], revealing the highest damage concentration at a depth of 1.4 μm, accompanied by distinct constants outlined in table 1.

Table 1. Parameters of Ni^{3+} ion irradiation

Ion irradiation conditions	
Equipment	Tandem accelerator
Displacement threshold energy	40eV
Beam	Ni^{3+} (3.2MeV)
Damage rate	1.0×10^{-4}dpa/s
Temperature	RT

A specialized sample mounting apparatus was custom-designed for the purpose of accommodating tensile specimens used in irradiation studies conducted under various external tensile stress conditions [16]. This device was uniquely tailored for integration into a tandem accelerator's beam line, enabling the irradiation of tensile samples at specific temperatures and affording meticulous regulation of applied stresses via load control.

2.3 Vickers hardness test

Using a Vickers HMV-1-SNJ modeled instrument, the Vickers hardness test was performed on non-irradiated samples. The load was exerted for a duration of 15 seconds during the 150.3 mN hardness assessment.

2.4 Nanoindentation test

Nano-indentation tests were conducted on tensile samples subjected to 1dpa irradiation at RT, utilizing an Elionix ENT-1100 machine equipped with a Berkovich type indenter. The indenter load (L) was adjusted to 1000 mgf, and the displacement (d) was kept below 300 nm to measure the hardness of the ion-irradiated layer. The red dashed circle in Fig. 1(c) represents the indentation marks that were found after the test. The computer system continuously monitors L and d, which exhibit the relationship as shown by the Eq (1) [18].

$$\frac{L}{d} = A + Bd \quad (1)$$

Where A and B are material-dependent constants and are unaffected by the load or the indenter's displacement. Given as B is:

$$B\ (GPa) = 0.287\ Hv\ (MPa) \quad (2)$$

Hv is an abbreviation for Vickers hardness.

The hardness resulting from ion irradiation of Zircaloy-2 was evaluated by comparing the B values within the depth interval of 100 to 200 nm. This depth range was chosen since the peak of irradiation damage lies at a depth of about 1.4 m, which is 3-5 times deeper than the indentation depth employed in this investigation.

2.5 TEM observation

The TEM specimens were obtained from the center part of the tensile samples. To achieve this, the center point of the tensile sample was marked using the dimple machine, ensuring that its thickness was significantly smaller than other areas, making it the preferred location for the twin-jet electro polisher to create pores. Following this, TEM specimens were meticulously prepared using the Struers TenuPol-5 twin-jet electro polisher. The specimen preparation involved utilizing a solution composed of 5% $HClO_4$ + 95% C_2H_5OH, carried out at a temperature of -55 °C and an applied voltage of 19 V.

To conduct characterization, the samples underwent analysis utilizing a JEOL JEM-2000EX electron microscope, which operated at 200 kV.

3. RESULTS AND DISSCUSSION

3.1 Impact of external tensile stress on hardness

Figure 2 illustrates the stress-strain curve of Zircaloy-2 at RT. The specimens were tested at a loading rate of 10 N/min. For this study, irradiation under stress conditions required maintaining the applied stress for approximately 1 hour to achieve an irradiation dose of 1 dpa. To ensure the sample did not undergo failure or fracture during the irradiation process, the applied stress level was carefully selected as highlighted by the blue arrows in Figure 2.

Vickers hardness testing was used to determine the impact of external tensile stress conditions on the hardness of unirradiated samples, as shown in Fig. 3.

The red error bars denote the associated standard deviation from the mean for each stress situation, and the black dots reflect the average hardness values acquired from several measurements.

The influence of diverse external tensile stresses on material hardening is negligible at room temperature. This outcome can be rationalized by the fact that the material remains primarily within the elastic deformation phase, resulting in minimal work hardening. This conclusion is congruent with the stress-strain diagram represented in Figure 2.

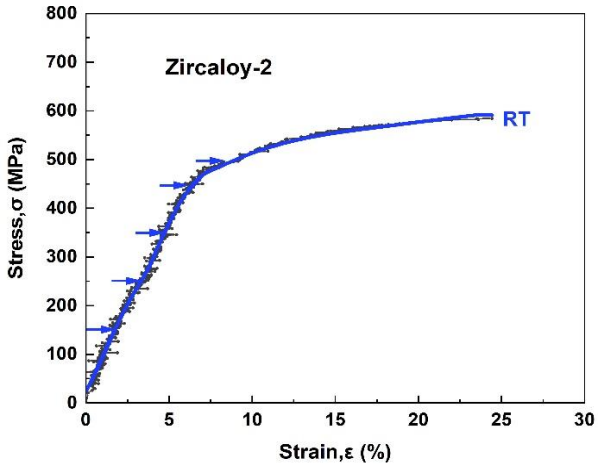

Fig. 2 Typical stress-strain curve of Zry-2 used at RT

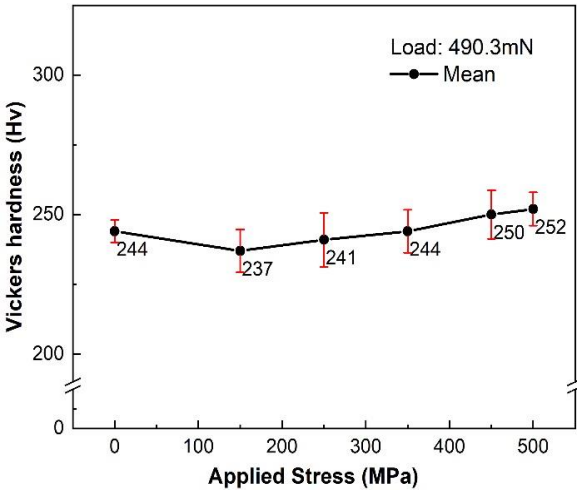

Fig. 3 Impact of external tensile stress on Vickers hardness of Zry-2 following 1-hour holding

3.2 Impact of external tensile stress on microstructure evolution

Fig. 4 illustrates the stress dependence of microstructure evolution in Zircaloy-2 subsequent to a 1-hour holding at RT. The externally applied stress direction is parallel to the observation plane. The micrograph at 0 MPa reveals annealed samples with a pristine interior and an exceptionally low dislocation density. Furthermore, the micrographs depict an assortment of precipitates, present both in the presence and absence of stress. Previous studies on zirconium alloys precipitates suggest that these may correspond to relatively large $Zr_2(Fe,Ni)$ precipitates, indicated by the orange arrows, with a size larger than 30 nm, as well as small $Zr(Fe,Cr)_2$ precipitates, shown as blue arrows [19-21].

When the externally applied stress was below 350 MPa, no dislocation lines were observed in the observation area. However, when the applied stress exceeded 450 MPa, dislocation lines induced by deformation were observed within some grains in the central part of the unirradiated tensile sample. Nevertheless, the density of dislocation lines varied significantly between different locations and within individual grains, which led to no significant increase in hardness values, as shown in Fig. 3.

The appearance and orientation of dislocation lines are correlated with the hcp structure of zirconium alloys and the direction of applied stress. Furthermore, as the dislocation density increases, different types of dislocation interactions occur, influencing the material's plastic deformation, hardness, and fracture behavior. By further increasing the externally applied tensile stress, plastic deformation occurs within the material, leading to an increased density of internal dislocations. This, in turn, enhances the interaction between dislocation loops generated by irradiation and those formed due to plastic deformation. Such investigations are valuable in understanding the influence of irradiation hardening effects during irradiation.

3.3 Irradiation-induced hardness under applied stresses

Fig. 5 depicts the stress recording process during the irradiation. Fig. 5(a) shows the plan for the stress control system with load adjustment, employing a loading rate of 10 N/min during the loading process. Once the applied stress reaches the target value, it will be held constant until the desired irradiation dose of 1 dpa was achieved. Fig. 5(b)-(f) present the actual stress recording process under different stress conditions during irradiation, providing detailed information about the irradiation conditions, including vacuum, beam currents during irradiation, and the sample displacement at the end of irradiation.

For samples subjected to lower applied stresses (below 450 MPa), the displacement during irradiation keep the same value. However, for samples with 500 MPa of applied stress, the displacement increased during the irradiation process. Notably, the recorded process corresponds to samples that did not fracture after multiple experiments. Due to the prolonged duration required to

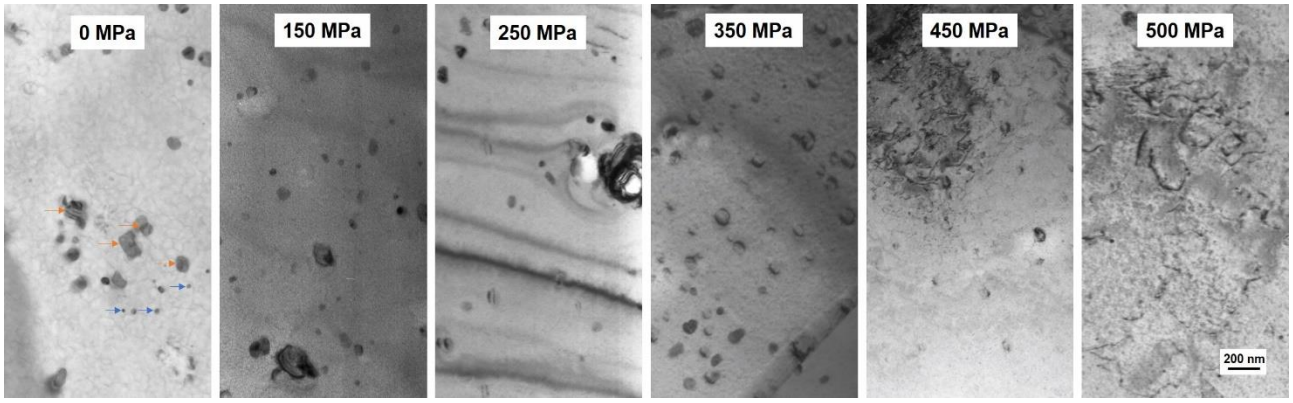

Fig. 4 Impact of external tensile stress on microstructure of Zry-2 following 1-hour holding

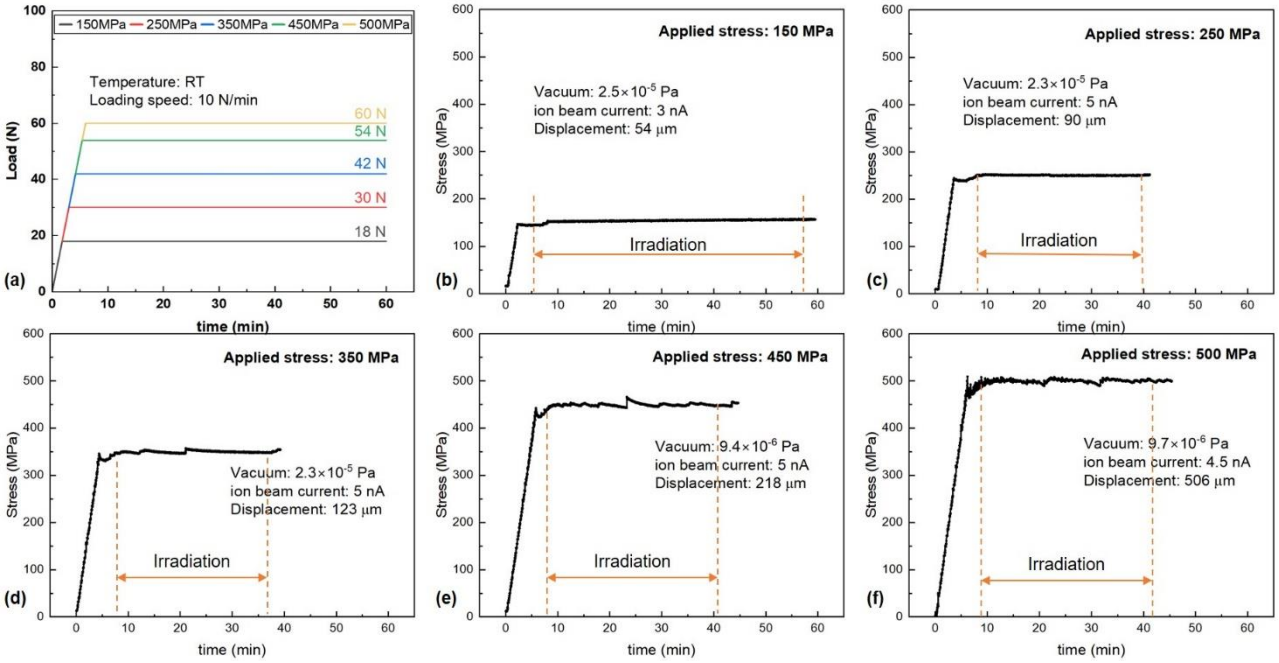

Fig. 5 (a) Stress control system, and (b)-(f) stress recording with different applied stress during ion irradiation

maintain 500 MPa applied stress during irradiation, some samples fractured during the irradiation process.

Throughout the irradiation process, minor fluctuations in actual stress are observed, but they consistently remain within 5% of the target value. This recording also indicates that the irradiation heating effect is not significant, as the stress control system is sensitive and would display larger fluctuations in stress if there were substantial changes in sample temperature. The reliable control of stress conditions during irradiation provides confidence in the experimental data and ensures the accuracy of the results obtained in this study.

Table 2. Hardness test of unirradiated and irradiated samples under different applied stresses

No.	Applied stress/MPa	ΔHv unirradiated	σ	ΔHv irradiated	σ
T1	150	-6.9	8.7	44.2	41.7
T2	250	-2.5	10.5	43.2	38.5
T3	350	0	8.7	55.4	44.3
T4	450	6.3	9.6	48.7	45.3
T5	500	8.6	7.2	58.8	53.3

Table 2 presents the changes in hardness under different applied stress conditions for both unirradiated and irradiated samples. For the unirradiated samples, the values represent the difference in Vickers hardness tested by Vickers hardness test before and after maintaining the applied stress for 1-hour at RT. On the other hand, for the irradiated samples, the values represent the change in Vickers hardness before and after irradiation, which were obtained from nanoindentation measurements and then converted to Vickers hardness. The table also includes the average values and standard errors obtained from multiple experiments, ensuring the reliability and accuracy of the data.

Utilizing data from Table 2, Figure 6 elucidates the impact of external tensile stress on the alteration in nano-hardness subsequent to exposure to 1 dpa irradiation at RT. Following the receipt of 1 dpa radiation at RT, the blue columns illustrate radiation-induced hardening at varying external tensile stress values. In addition, the white columns depict the stress-induced variations in hardness observed in non-irradiated samples tested by Vickers hardness test subjected to equivalent stress conditions. The standard deviation from mean of radiation-induced hardness for each stress condition is represented by black error bars, while the standard deviation of external tensile stress-induced hardness is indicated in red for each stress condition.

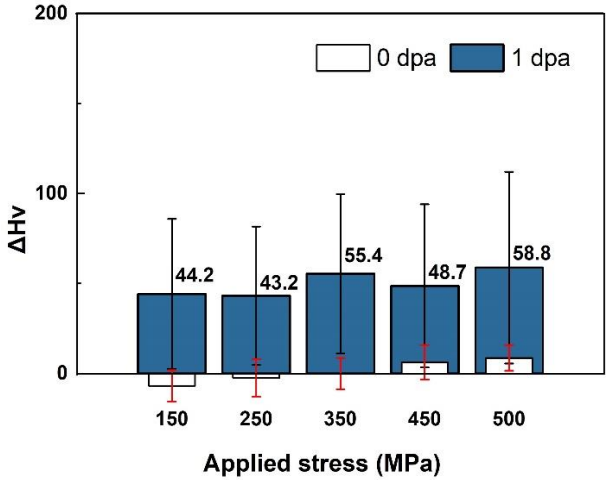

Fig. 6 Impact of external tensile stress on irradiation-induced and stress-induced hardness in 1 dpa irradiated Zry-2 at RT

Under the same stress conditions, the irradiated samples show a significant increase in hardness, approximately 50 Hv. This phenomenon can be traced to the formation of <a> type dislocation loops, a key factor contributing

to irradiation hardening in Zr alloys, as indicated by previous research [10, 11, 22]. <a> loop is a type of dislocation loop that forms due to the interaction between irradiation-induced vacancies and self-interstitial atoms (SIA) in the Zr lattice. When high-energy particles displace atoms from their lattice sites, vacancies are created, and these vacancies can then migrate and interact with self-interstitial atoms, resulting in the formation of <a> loops.

The presence of <a> loops in the Zr lattice results in interactions between dislocations and <a> loops, which hinder dislocation movement and lead to an increase in material hardness. Consequently, the material becomes stronger and more resistant to deformation due to the presence of these <a> loops. The understanding of the role of <a> loops in irradiation hardening is crucial for predicting the mechanical response of Zr alloys under irradiation conditions and for designing materials with enhanced performance in nuclear reactor environments [23-24].

However, for various applied stress levels, the increase in hardness values after 1 dpa irradiation is similar, indicating that the influence of stress is not pronounced. This observation is consistent with the results shown in Fig. 3, where the effect of different applied stresses on material hardening at room temperature below 500 MPa is not significant.

In the case of irradiation carried out with external tensile stress, irradiation hardening can be explained by a number of causes, including hardening brought on by the introduction of dislocations as a result of the external tensile stress, work hardening brought on by irradiation-induced <a> type dislocation loops, and hardening due to the interaction between dislocations produced by external tensile stress and dislocations produced by irradiation.

The applied stress has no impact on the hardness of the unirradiated sample at RT. Furthermore, with 1.0 dpa irradiation at RT, the change in hardening caused by the external tensile stress is not significant. Similar conclusions were drawn by Watanabe et al. [16] in their investigation of stress's influence on irradiation hardening in Fe-Mn alloys. They determined that stress application had no discernible effect on the increase in irradiation-induced hardness.

Further investigation with higher applied stress levels and microscopic analysis of irradiated samples under stress conditions are necessary to gain a further knowledge of the underlying mechanisms and to explore potential synergistic effects between stress and irradiation on material hardening.

4. CONSLUSIONS

The ongoing study examines the impact of external tensile stress on the microstructure of Zry-2 following a 1-hour holding duration and the influence of 3.2 MeV Ni^{3+} irradiation on the radiation-induced hardness of Zircaloy-2 at room temperature, considering varying levels of applied stress. The obtained results can be summarized as follows:

Firstly, at room temperature, the samples were subjected to different levels of applied stress ranging from 150 MPa to 500 MPa and were held under stress for a duration of 1 hour. Vickers hardness testing revealed that the applied stress below 500 MPa at room temperature had no significant impact on the hardness values of the unirradiated samples. This is because the material remained in the elastic deformation stage below 500 MPa at room temperature, where no significant work hardening occurs.

Secondly, for the 1 dpa irradiated samples with stress conditions at room temperature, a considerable increase in hardness of approximately 50 Hv was observed, indicating significant hardening. This phenomenon can ascribe to the formation of <a> loops, in line with prior research findings [13].

Moreover, the applied stress did not show a substantial influence on the hardening caused by 1.0 dpa irradiation at room temperature. This finding is consistent with some previous researches on the effect of stress in irradiation hardening of Fe-based alloys. To observe a more pronounced effect of stress, it may be necessary to use samples that have undergone cold work prior to irradiation. This would allow the material to withstand higher stresses during irradiation while maintaining the high density of dislocations during the irradiation.

Further TEM characterization is necessary to comprehensively examine the dislocation loops generated due to irradiation and those influenced by external tensile stress. This is particularly crucial for irradiated samples subjected toexternal stress, as it would contribute to a more comprehensive understanding of the intricate interplay between stress and irradiation. This microscopic analysis will provide valuable insights into the underlying mechanisms and contribute to a deeper comprehension of the irradiation hardening behavior in Zircaloy-2 under stress conditions.

5. REFERENCES

[1] S. J. Zinkle, G. S. Was, Materials Challenges in Nuclear Energy, Acta Materialia, 61 (2013) 735–58.

[2] Masafumi Nakatsuka, Mechanical Properties of Neutron Irradiated Fuel Cladding Tubes, Journal of Nuclear Science and Technology, 28 (1991), 356–68.

[3] A. T. Motta, A. Couet, and R. J. Comstock, Corrosion of Zirconium Alloys Used for Nuclear Fuel Cladding, Annual Review of Materials Research, 45 (2015) 311–343.

[4] Z. Yao, M. Daymond, S. Di, and Y. Idrees, Irradiation Induced Defect Clustering in Zircaloy-2, Applied Sciences, 7 (2017) 854.

[5] N. Gharbi, F. Onimus, D. Gilbon, J.-P. Mardon, and X. Feaugas, Impact of an applied stress on c-component loops under Zr ion irradiation in recrystallized Zircaloy-4 and M5®, Journal of Nuclear Materials, 467 (2015) 785–801.

[6] B. Ensor, A. T. Motta, A. Lucente, J. R. Seidensticker, J. Partezana, and Z. Cai, Investigation of breakaway corrosion observed during oxide growth in pure and low alloying element content Zr exposed in water at 360°C, Journal of Nuclear Materials, 558 (2022) 153358.

[7] W. Qin, J. L. Liang, Z. Q. Cheng, M. H. Shi, D. Gu, T. L. Li, W. L. Zhu, J. A. Szpunar, Threshold stress of hydride reorientation in zirconium alloy nuclear

fuel cladding tubes: A theoretical determination, Journal of Nuclear Materials, 563 (2022) 153659.
[8] A. V. Barashev, S. I. Golubov, and R. E. Stoller, Theoretical investigation of microstructure evolution and deformation of zirconium under neutron irradiation, Journal of Nuclear Materials, 461 (2015) 85–94.
[9] G. J. C. Carpenter, R. H. Zee, and A. Rogerson, Irradiation growth of zirconium single crystals: A review, Journal of Nuclear Materials, 159 (1988) 86–100.
[10] H. L. Yang, S. Kano, J. McGrady, D. Y. Chen, K. Murakami, and H. Abe, Microstructural evolution and hardening effect in low-dose self-ion irradiated Zr–Nb alloys, Journal of Nuclear Materials, 542 (2020) 152523.
[11] Q. Dong, H. Qin, Z. Yao, and M. R. Daymond, Irradiation damage and hardening in pure Zr and Zr-Nb alloys at 573 K from self-ion irradiation, Materials & Design, 161 (2019) 147–159.
[12] Y. Idrees, Z. Yao, M. A. Kirk, and M. R. Daymond, In situ study of defect accumulation in zirconium under heavy ion irradiation, Journal of Nuclear Materials, 433 (2012) 95–107.
[13] L. Xue, H. Watanabe, Radiation-induced hardening of ion-irradiated Zircaloy-2 at 573 K under applied stress, Nuclear Instruments and Methods in Physics Research Section B: Beam Interactions with Materials and Atoms, 542 (2023), 223-229.
[14] Y. Wang, K. Hanada, Y. Hu, K. He, Guiding center orbit simulation of energetic particles in tokamak plasma, Proceedings of International Exchange and Innovation Conference on Engineering & Sciences (IEICES), 8 (2022) 228-233.
[15] M. J. Kobra, G. Watanabe, Y. Yamaguchi, Y. Uozumi, Extension of intranuclear cascade model for deuteron- and alpha-induced reactions, Proceedings of International Exchange and Innovation Conference on Engineering & Sciences (IEICES), 3 (2017) 175-178.
[16] H. Watanabe, A. Hiragane, S. Shin, N. Yoshida, and Y. Kamada, Effect of stress on radiation-induced hardening of A533B and Fe–Mn model alloys, Journal of Nuclear Materials, 442 (2013) S776–S781.
[17] Ziegler ZF. SRIM–The Stopping and Ranges of Ions in Matter. http://www.strim.org
[18] M. Inamura, T. Suzuki, Evaluation of materials strength by Ultra-Micro-Indentation, Seisan Kenkyu, 42 (1990) 257-260.
[19] H. Watanabe, K. Takahashi, K. Yasunaga, Y. Wang, Y. Aono, Y. Maruno, K. Hashizume, Effects of an alloying element on a c-component loop formation and precipitate resolution in Zr alloys during ion irradiation, Journal of Nuclear Science and Technology, 55 (2018) 1212–1224.
[20] J. Bowman, P. Wang, G. S. Was, M. Bachhav, and A. T. Motta, Ion irradiation induced amorphization of precipitates in Zircaloy, Journal of Nuclear Materials, 571 (2022) 153988.
[21] M. Griffiths, A review of microstructure evolution in zirconium alloys during irradiation," Journal of Nuclear Materials, 159 (1988) 190–218.
[22] H. Yang, Anisotropic effects of radiation-induced hardening in nuclear structural materials: A review, Journal of Nuclear Materials, 561 (2022) 153571.
[23] Z. Yao, M. Daymond, S. Di, and Y. Idrees, Irradiation Induced Defect Clustering in Zircaloy-2, Applied Sciences, 7 (2017) 7080854.
[24] M. Griffiths, M. H. Loretto, and R. E. Smallman, Electron damage in zirconium: I. defect structure and loop character, Journal of Nuclear Materials, 115 (1983) 313–322.